sciendo

Management Systems in Production Engineering

2024, Volume 32, Issue 4, pp. 548-554

Date of submission of the article to the Editor: 05/2024
Date of acceptance of the article by the Editor: 10/2024

DOI 10.2478/mspe-2024-0052

DECISION SUPPORT SYSTEM FOR THE DESIGN PROCESS OF APATITE BIOPOLYMER COMPOSITE PARTS

Anton Panda
Technical University of Kosice

Kostiantyn Dyadyura, Dmitriy Dmitrishin, Andrey Smorodin, Igor Prokopovich
Odesa Polytechnic National University

Abstract:
In connection with the increase in the number and severity of various types of bone tissue injuries received as a result of wounds during military operations in Ukraine, an important issue in orthopedics and traumatology is making informed decisions about the possibility of restoring the integrity and functions of bone tissue when using different types of composition, porosity and strength of apatite-biopolymer composites. The scientific direction of research is the development of principles and methods for making scientifically based decisions in the design and additive manufacturing of bone substitutes based on apatite-biopolymer composites with functional properties depending on the nature of the localization of the cavity bone defect and its size. A set of methods for analyzing images of bone tissue, taking into account its spatial structure, which are obtained by sensors of different physical nature, with the use of neural network models, development of methods of their design, optimization and training is proposed. The new knowledge obtained as a result of the project will become the necessary basis for making optimal decisions in practice for the introduction of the latest methods of treatment and prosthetics in trauma surgery, oncology, cranio-maxillofacial surgery, dentistry, taking into account the risks of biocompatibility of apatite-biopolymer composites. Software development of an intelligent decision support system will be used to design bone substitutes with controlled composition, structure, porosity and mechanical strength for the further selection of additive technology for its production from apatite-polymer composites, which will contribute to increasing the efficiency of treatment and prosthetics in orthopedics and traumatology.

Key words: deep learning-based neural network application, apatite biopolymer composites, 3D printing, tissue engineering, medical devices, drug delivery, bone scaffolds, additive manufacturing

INTRODUCTION

The use of bone substitutes with functional properties that take into account the patterns of new formation of bone tissue has become possible thanks to the use of the CAD/CAM/CAE system of design and additive technologies [1]. Making informed decisions in the design of bone substitutes for their additive manufacturing, taking into account all risks, is possible only on the basis of the results of image analysis, which are highly effective in terms of accuracy and speed, obtained when using modern methods of radiography, computer and magnetic resonance imaging, etc. [2]. Deep learning methods, in particular generative models, have gained significant popularity in the analysis of medical images [3]. For the additive manufacturing of bone substitutes with controlled composition, structure, porosity and strength depending on the nature and localization of the hollow bone defect, its size and loading conditions, a complex of interrelated methods and means of analysis, clustering, segmentation and classification of objects in images is proposed [4]. At the heart of these methods are various geometric or pixel transformations that can allow the generation of images similar to the original ones [5]. Such technologies are particularly relevant in maxillofacial surgery for the restoration of mild or serious facial disfigurement along with numerous and unpredictable functional disorders. The lower jaw is one of the most important anatomical structures responsible for various functions and aesthetic properties in the head and neck region. The problems associated with the management of the patient after mandibulectomy depend on many factors, such as the size of the defect, the location of the arch, and the adjacent structures lost. Technologies

© 2024 Author(s). This is an open access article licensed under the Creative Commons BY 4.0 (https://creativecommons.org/licenses/by/4.0/)

and methods of medical image analysis and additive manufacturing make it possible to obtain an accurate model of tissue defects of the lower jaw for reconstructive surgery. This allows to significant increase the success rate of prosthetics and improves the quality of life of such patients. Successful orthopaedic rehabilitation involves understanding the altered function of the mandible and the possible treatment options available to meet the patient's individual needs. The relevance of the research presented in this paper is that the development of an intelligent decision support system will allow the creation of three-dimensional solid models of defects of the lower jaw taking into account its spatial structure for the production of bone substitutes with controlled composition, porosity and mechanical strength of biomaterials. Such bone substitutes will be optimal for a specific area of damaged tissue of the lower jaw, which will increase the effectiveness of treatment of such diseases.

The purpose of the research is to create a decision-making support system for the analysis of images of bone tissue defects of the lower jaw, taking into account its spatial structure, which is obtained by sensors of different physical nature, based on the use of neural network models, the development of methods for recognizing the region of interest (Region of Interest) in the image, optimization and training.

LITERATURE REVIEW

Maxillofacial defects lead to a variety of physical and emotional reactions in the patient and can be emotionally traumatic. The success of the rehabilitation of such patients depends on the strategic planning of the treatment and the choice of the most suitable method of treatment. Mandibular bone mainly consists of inorganic components (hydroxyapatite) associated with hardness and organic components (collagen) associated with elasticity [6]. Requirements for the structure of bone substitutes (variations in chemical composition, porosity, pore size, shape and their network) compliance with the specific form of the defect. Accordingly, a wide selection of implant materials is available for mandibular reconstruction, including bioceramics made of calcium phosphate components [7, 8, 9]. Bioceramics have excellent osteoconductivity, which is useful for the regeneration of the lower jaw bone. However, the fragility limits the application for large defects [10, 11], the framework for mandibular reconstruction, especially with complex anatomical structures, including curvature, and condyle, and needs a combination of bioceramics, synthetic and natural polymers that can complement their defects. The use of osseointegrated implants provides stable fixation for the installation of dentures on implants even in the absence of an alveolar ridge. Anatomically selected osseointegrated implants have very complex geometric contours and forms. Prosthodontic success in mandibular resection patients is closely related to accurately locating certain elements in the image to not only know where they are but also to visualize their shape. Major factors affecting accuracy are image resolution, amount of image noise, the contrast between tissues of interest, and artefacts inherent in the imaging system.

Medical image segmentation involves the extraction of regions of interest (ROI) from medical images. Many segmentation algorithms can be found in the literature [12, 13, 14]. There is a wide range of algorithms for solving segmentation problems [15]. In recent years, segmentation and classification of images with the help of convolutional neural networks have gained great popularity [16, 17, 18]. Each of the image segmentation methods has its advantages and disadvantages. Currently, there is no single segmentation technique that is suitable for all images and applications. Against this background, the widespread success of deep learning (DL) has prompted the development of new image segmentation approaches using DL models.

In recent years, several platforms have appeared in the artificial intelligence community that contribute to the development of deep learning neural networks for medical visualization [19, 20, 21]. A review of the works of such authors as Akazawa and Hashimoto [22], De Siqueira, etc. [23], Fernando et al. [24], Chen et al. [25], Sah and Direcoglu [26] and Abdu [27] showed that convolutional neural networks are capable of exploiting local and global features of medical images, and they can also be trained to utilize 3D image information. UNet is considered as one of the most popular and general architectures for the segmentation of medical images [28]. With models like U-Net, which generate an image from an existing one, it is possible to analyze each pixel of an input image, classifying them according to the object they are a part of.

The main problem of segmentation of medical images remains the high variability of shape, location, size and texture of medical images. The task of segmentation of medical objects is solved by defining the area under investigation (ROI). The choice of regions to be studied is different for different image analyses. It is often impossible to collect a sufficient number of images and prepare a high-quality set of data certified by doctors. The existing automated methods of ROI detection [29] do not provide sufficient accuracy and reliability. This implies the need for a separate and reliable method for ROI detection.

RESEARCH METHODOLOGY

In this study, a technique for identifying diagnostically significant areas under investigation was developed to support decision-making in automated image analysis of bone tissue defects of the lower jaw based on pattern recognition algorithms.

Pattern recognition algorithm

We describe an image by an N-dimensional vector q, the individual components of which are features encoded using numbers. We also assume that the number M of prototypes of images is given and can be represented by state vectors.

$$V^{(k)} = \begin{pmatrix} v_1^{(k)} \\ \cdots \\ \cdots \\ v_N^k \end{pmatrix}, \quad (1)$$

where:
index *k* takes values from 1 to M.
Depending on the number of vectors $V^{(k)}$, their linear span coincides either with the entire feature space or with its subspace. In the latter case, additional ("extra") vectors have to be introduced. Samples (1) form a database. When an image is presented that needs to be recognized due to noise, incomplete data (absence of certain features), etc. this image may not coincide with any of the vectors (1), but it may be close enough to one of the prototype images, i.e. to one of the axes of the feature space. Our main idea boils down to the following: let's agree to describe the presented image by vector *q(0)*, where argument 0 refers to the initial time *t* = 0 of the pattern recognition process. We then need to find equations for the time-dependent vector *q(t)* that describe the evolution of this vector from the initial state *q(0)* to the final state q_f, consistent with one of the prototype vectors $V^{(k)}$.
We will construct these equations in such a way that the vector $V^{(k)}$, in question, is the very vector to which the vector *q(0)* comes closest, i.e. the quantity $\left(V^{(k)^+} \cdot q(0)\right) / \left(\left|V^{(k)}\right| \cdot |q(0)|\right)$ (1) had the smallest value. We assume that $(V^{(k)+} \cdot V^{(k')}) = \delta_{kk'}$. Thus, if the initial image is incomplete, it can be supplemented, i.e. the algorithm acts as an "associative memory." The equations that help to accomplish all things are as follows:

$$q' = -grad_q P + F(t), \quad (2)$$

The potential *P* entering into them is determined by the equation

$$P(q) = P_0 + P_1 + P_2, \quad (3)$$

where:

$$P_0 = -\frac{1}{2} \cdot q^+ \cdot \sum_k \lambda \cdot V^{(k)} \cdot V^{(k)+} \cdot q, \quad (4)$$

$$P_1 = \sum_{k \neq k'} C_{kk'} \left(V^{(k)+} \cdot q\right)^2 \cdot \left(v^{(k')+} \cdot q\right)^2, \quad (5)$$

$$C_{kk'} > 0, \quad (6)$$

$$V_2 = C \cdot q^4 \quad (7)$$

The term V_0 "pulls" the vector *q* into the subspace spanned by the prototypes of the images. In the language of the theory of non-equilibrium phase transitions, this is simply a space of order parameters. The computational difficulties associated with the solution can be reduced if subsequent decisions are made in the feature space of a lower dimension. The use of information has one peculiarity: the greater the dispersion of eigenvalues λ_i, the less the entropy, the greater the reduction of information. On the contrary, when the eigenvalues λ_i are uniformly distributed in magnitude, we have strong uncertainty and large entropy.
The term V_1 serves to discriminate vectors q in the space of image prototypes. This can be verified by using the property that the minimum of the function V_1 is selected in accordance with the condition

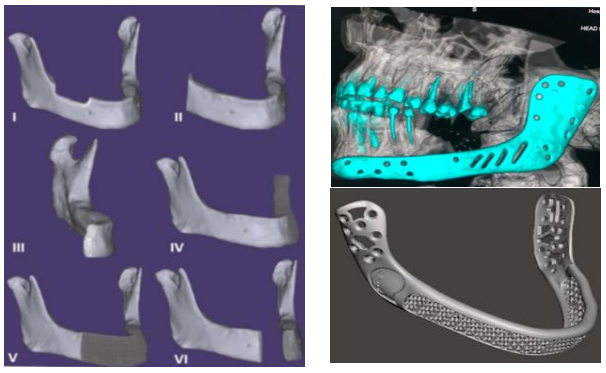
$$V_{1,min} = 0 \; at \; q || V^{(k_0)} \quad (8)$$

i.e. when the state vector q becomes parallel to one of the prototype vectors and thus the initial vector of state *q*(0) is identified with the corresponding image prototype.
Finally, the V_2 term provides saturation, i.e. value |q| eventually is attracted to the attractor – a fixed point on the $V^{(k_0)}$ axis. The constant λ in relation (3) is a control parameter: $\lambda < 0$ defines the region below the "threshold", $\lambda > 0$ defines the region above the threshold. In this research we will assume that $\lambda > 0$. So, the vector q must be brought to coincide with one of the vector prototypes. To simplify this operation, we have added a fluctuating force *F* to equations (3). As usual, we assume that the fluctuating forces have the following properties:

$$\langle F(t) \rangle = 0, \quad (9)$$

$$\langle F_i(t) \cdot F_j(t') \rangle = Q \cdot \delta_{ij} \cdot \delta(t - t') \quad (10)$$

Our pattern recognition approach was verified through a numerical experiment. The Cantor and Curtis classification of intraoral defects of the lower jaw [30, 31]: radical alveolectomy with preservation of mandibular continuity (I); lateral resection of the mandible distal to the cusp area (II); lateral resection of the mandible to the midline (III); lateral bone graft and surgical reconstruction (IV); anterior bone graft and surgical reconstruction (V); and anterior mandibular resection without surgical reconstruction (VI) (Figure 1) was taken as a basis, which developed its basis for directing surgical and prosthetic rehabilitation.
Defects were converted into digital form, for which the image was divided into a square grid measuring 60x60 cells. Each cell corresponds to a component of the vector $V^{(k)}$. The program for solving equation (2) was presented with a test sample *q* in the form of a part of a person's face. By passing from the vectors $V^{(k)}$ and *q* to their Fourier images and using the absolute values of the Fourier images as new variables, the entire process of pattern recognition was reduced to invariants under translations.
Learning is reduced to optimization (minimization) of loss functions. The main function optimization method used is the Stochastic Gradient Descent (SGD) method, which is an iterative algorithm that follows a function until it finds its lowest point as gradient descent.



a) ***b)***

Fig. 1 Image prototypes: a) the intraoral mandibular defects, classified according to Cantor and Curtis classification in six classes; b) implant models for replacing damaged lower jaw

Based on the analysis of existing GNM training methods, which are included in modern neural network development libraries, it was found that most of them are based on the gradient descent method, which in the mini-batch training mode formally looks like this:

$$\Theta_{t+1} = \Theta_t - \frac{1}{B} \cdot \gamma \cdot \nabla_{\Theta} \cdot \sum_{i=1}^{B} L(f(\bar{x}_i; \Theta_t), \bar{y}_i), \quad (11)$$

where:
Θ_t neural network parameters at time t;
B is the number of elements in one mini-packet of training data;
$L(f(\bar{x}_i; \Theta_t), \bar{y}_i)$ is a loss function that reflects the error between the predicted values $f(\bar{x}_i; \Theta_t)$ and the expected results $\bar{y}_i$;
$f(\bar{x}_i; \Theta_t)$ is a function denoting the corresponding transformations performed by a neural network with internal parameters Θ_t and input parameters.
If you enter an additional function from the ϑ parameter:

$$G(\vartheta) = \vartheta - \frac{1}{B} \cdot \gamma \cdot \nabla_{\vartheta} \cdot \sum_{i=1}^{B} L(f(\bar{x}_i; \vartheta), \bar{y}_i) \quad (12)$$

Then the expression (11) can be represented in the form of a classical discrete dynamic system (DDS) [32]

$$\Theta_{t+1} = G(\Theta_t) \quad (13)$$

In practice, they use a set of loss functions (objective functions), specially created for different classes of tasks. The task of neural network training is reduced to finding the minimum of the loss function. So, the entire learning process can be imagined as a standard optimization problem that can be solved by known optimization methods. The set of these methods can be divided into two large classes: first and second order. The difference between the classes lies in the degree of the derivative of the objective function used for optimization. The research flow diagram is shown in Fig. 2. The beginning of image creation is the collection of raw image data. It collects raw information about the inside of the human body and becomes the main focus of all subsequent image processing tasks. Ultimately, regardless of the image format, the data acquisition process detects physical factors, preprocesses the collected signals, and then digitizes them (see Figure 2).

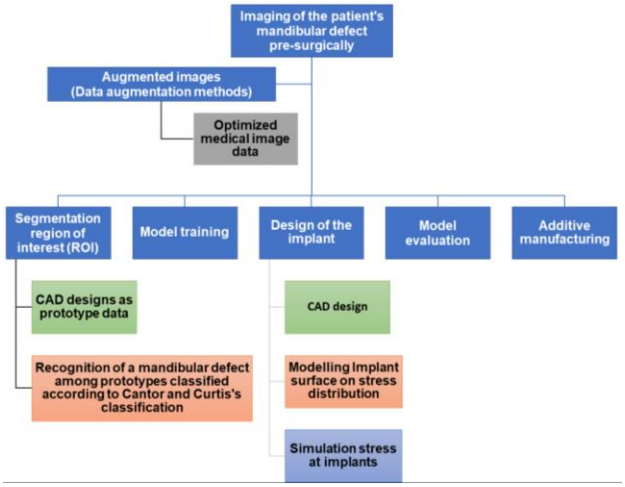


Fig. 2 Flowchart of the process from medical imaging to additive manufacturing lower jaw for reconstructive surgery

RESULTS

The results of the research are shown in Figures 3-8. The process of research can be divided into eight stages:

1) The stage of receiving images. At the stage of image acquisition, medical images are obtained from medical CT imaging devices (Figure 3).



Fig. 3 Patient B Diagnosis: Ameloblastoma of the lower jaw

2) The stage of segmentation. In the segmentation phase, the obtained medical images are segmented according to the design objective and processed for separation (segmentation) to extract a subset that will represent the part of the anatomy under consideration (Figure 4).



Fig. 4 Segmentation of the acquired medical image according to objectives to identify a subset that will represent part of the anatomy in question

3) The stage of 3D modeling. At the stage of 3D modeling, the segmented data representing the bone tissue are transformed (reconstructed) into a 3D model optimized for 3D printing (Figure 5).

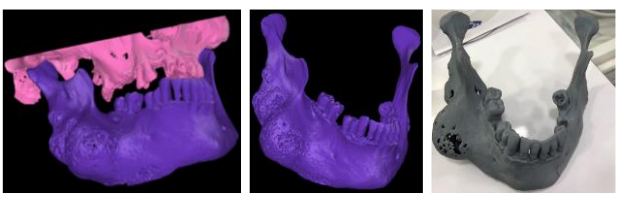


Fig. 5 3D modeling and printing of the model for preoperative preparation

4) The stage of 3D printing. 3D printing is done using a developed 3D model. For this step, the 3D model is processed for 3D printing by slicing, assigning build parameters, orienting and placing it in the build space, and may also have support structures created (Figure 6).

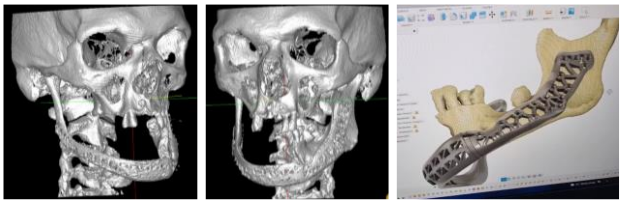


Fig. 6 The model was evaluated against various criteria and produced excellent predictions on test images

5) The stage of post-processing. In the post-processing step, the 3D printed part undergoes post-processing to become suitable for actual medical use (Figure 7).

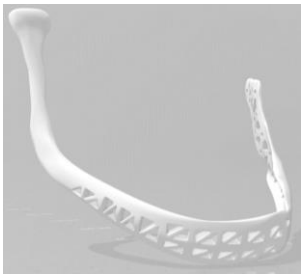


Fig. 7 Additive manufacturing implant for reconstructive surgery from apatite biopolymer composites

6) The stage of quality control (QC). In the QC phase, the 3D-printed part is finally checked against all requirements (user/design/quality/risk).
7) The stage stage of clinical application and review. At the stage of clinical application and examination, a medical professional checks the 3D printed part as suitable for clinical use (Figure 8).

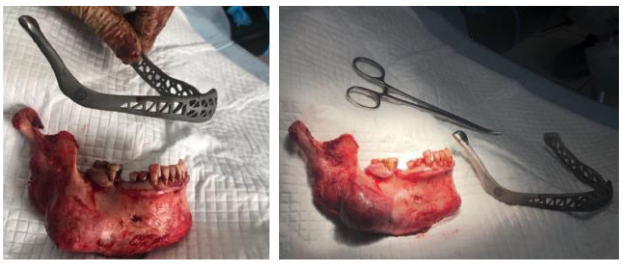


Fig. 8 Surgery to remove the tumor and install an implant

In this study, the contextual region of interest (CROI) was expanded based on the difference between the intensity of a pixel and the average value of other pixels in the same row. The obtained results were analyzed using CR, MSE, PSNR, and CoC metrics, and compared with general methods such as JPEG, JPEG2K, and SPIHT, as well as ROI-based methods such as Maxshift, EBCOT, and CSPIHT. After preparing the raw data, the main part of the system was built on the basis of the new Pytorch Lightning library, developed on the basis of PyTorch to facilitate development and research in deep learning. The advantage of this library is its ability to parallelize the training process not only between several cores of the same processor and/or several graphic accelerators on the same server, but also to use different architectures of distributed computing (including "cloud" solutions of Amazon, Azure and Google). The training process was performed on a computer with an integrated GPU and took an average of about one hour for each optimizer. To get an initial idea of the learning characteristics for a given neural network architecture and generated training data, the recommended Adam algorithm was applied with a learning factor of 0.0001. Several runs for 100 epochs showed that the network stops learning quite quickly, which means that it does not make sense to spend so much time and resources, so it was suggested to limit ourselves to 50 epochs for comparison.

Thus, during the creation of an intelligent decision-making system, the main advantage in this work is not the original architectural approach to neural networks, but the development of a new method for recognizing the studied regions of interest (ROI) from medical images.

DISCUSSION

In the future we will also be interested in another aspect of ROI recognition. As a visual aid, we use the analogy between ROI recognition, which we describe using equation (2), and nonequilibrium phase transitions. Let us transform equation (2) of the Langevin equation type into the Fokker-Planck equation:

$$f' = \sum_k \frac{\partial}{\partial q_k}\left(\frac{\partial P}{\partial q_k}\cdot f\right) + \frac{Q}{2}\cdot\sum_k \frac{\partial^2 f}{\partial q_k^2} \tag{14}$$

The stationary solution has the form

$$f = N\cdot exp\left(-\frac{2P}{Q}\right) \tag{4}$$

Thus, the stationary phenomenon is completely determined by the potential *P* (equation 3) and the magnitude of fluctuations *Q*. The maximums of the solution $f(q)$ correspond to the minimums of the potential $P(q)$. As a simple analysis shows, the minima of the potential $P(q)$ are located at the points $q = V^{(k)}$, i.e. coincide with the prototype images. The above is true for eigenvalues $\lambda > 0$. As for the region $\lambda < 0$, the minimum of the potential in it is located at the point $q = 0$, i.e. even if the initial images are presented to the system, they will still disappear.

CONCLUSIONS

After the conducted research, the following scientific results were obtained, which are a significant contribution to the further improvement of decision-making methods in the analysis of images of bone tissue defects of the lower jaw, taking into account its spatial structure, which is obtained by sensors of different physical nature: an analysis of existing neural networks for solving the tasks of segmentation and classification of medical images was performed, which made it possible to choose and justify the choice of research direction; an analysis of the current state of gradient descent methods, which are used in solving practical tasks of segmentation and classification, was

performed; a method for recognizing regions of interest (ROI) was developed for the proposed classification of maxillofacial defects and implant structures.

The introduction of the new recognition method allowed to improve the resolution of the image, reduce the amount of noise in the image, increase the contrast between the interesting tissues and the artifacts that are inherent in the image of bone tissue of the jaw. New recognition methods were implemented in deep neural network training, where a 20% percent speedup in neural network training was achieved. The obtained theoretical results were tested in the additive manufacturing of a bone substitute for the treatment of ameloblastoma of the lower jaw. Further research will focus on learning and reproducing processes that are Markov. Further research will show that the decision-making system will self-adjust to optimized medical image data for additive manufacturing for medicine.

ACKNOWLEDGMENTS

This work was supported by the project VEGA 1/0226/21 of the Scientific Grant Agency of the Ministry of Education, science, research and sport of the Slovak Republic.

REFERENCES

[1] ISO/ASTM TR 52916:2022 "Additive manufacturing for medical – Data – Optimized medical image data", 2022.

[2] P. Celard, E.L. Iglesias, J.M. Sorribes-Fdez, R. Romero, A. Seara Vieira and L. Borrajo. "A survey on deep learning applied to medical images: from simple artificial neural networks to generative models". *Neural Comput & Applic.*, vol. 35, pp. 2291-2323, 2023.

[3] M. Bahraminasab. "Challenges on optimization of 3D-printed bone scaffolds". *BioMed Eng OnLine.,* vol. 19, 69, 2020.

[4] H.I. Park, J.H. Lee, and S.J. Lee. "The comprehensive on-demand 3D bio-printing for composite reconstruction of mandibular defects". *Maxillofac Plast Reconstr Surg*, vol. 44, 31, 2022.

[5] B. Zhang, Y. He, J. Liu, J. Shang, Ch. Chen, T. Wang, M. Chen, Y. Li, G. Gong, J. Fang, Z. Zhao and J. Guo. "Advancing collagen-based biomaterials for oral and craniofacial tissue regeneration". *Collagen & Leather*, vol. 5, 14, 2023.

[6] L. Sukhodub, A. Panda, K. Dyadyura, I. Pandova and T. Krenicky. "The design criteria for biodegradable magnesium alloy implants." *MM Science Journal,* 2018, 2018 (December), pp. 2673-2679, 2020.

[7] A. Panda, K. Dyadyura, J. Valíček, M. Harničárová, M. Kušnerová, T. Ivakhniuk, L. Hrebenyk, O. Sapronov, V. Sotsenko, P. Vorobiov, V. Levytskyi, A. Buketov and I. Pandová. "Ecotoxicity Study of New Composite Materials Based on Epoxy Matrix DER-331 Filled with Biocides Used for Industrial Applications". *Polymers*, vol. 14, no. 16, 3275, 2022.

[8] F. Camacho-Alonso, C. Martínez-Ortiz, L. Plazas-Buendía, A.M. Mercado-Díaz, C. Vilaplana-Vivo, J.A. Navarro, A.J. Buendía, J.J. Merino and Y. Martínez-Beneyto. "Bone union formation in the rat mandibular symphysis using hydroxyapatite with or without simvastatin: effects on healthy, diabetic, and osteoporotic rats". *Clin Oral Invest,* vol. 24, pp. 1479-1491, 2020.

[9] F. Ramzan, A. Salim and I. Khan. "Osteochondral Tissue Engineering Dilemma: Scaffolding Trends in Regenerative Medicine". *Stem Cell Rev and Rep,* vol. 19, pp. 1615-1634, 2023.

[10] L. Sukhodub, A. Panda, L. Suchodub, M. Kumeda, K. Dyadyura and I. Pandova. "Hydroxyapatite and zinc oxide based two-layer coating, deposited on Ti6Al4V substrate." *MM Science Journal,* 2019 (December), pp. 3494-3499, 2019.

[11] S.V.S. Prasad, B.Ch. Rao, M.K. Rao, K.R. Kumar, S.D.V. Prasad, Ch. Ramesh. "Medical image segmentation using an optimized three-tier quantum convolutional neural network trained with hybrid optimization approach". *Multimed Tools Appl*, vol. 83, pp. 38083-38108, 2024.

[12] N. Jitani, B.J. Singha, G. Barman, A. Talukdar, R. Sarmah and D.K. Bhattacharyya. "Medical image segmentation using automated rough density approach". *Multimed Tools Appl*., vol. 83, pp. 39677-39705, 2024.

[13] S. Minaee, Y. Boykov, F. Porikli, A. Plaza, N. Kehtarnavaz and D. Terzopoulos. "Image Segmentation Using Deep Learning: A Survey". *IEEE Trans Pattern Anal Mach Intell*, vol. 44, no. 7, pp. 3523-3542, 2022.

[14] S. Iqbal, A.N. Qureshi, J. Li, and T. Mahmood. "On the Analyses of Medical Images Using Traditional Machine Learning Techniques and Convolutional Neural Networks". *Arch Computat Methods Eng.*, vol. 30, pp. 3173-3233, 2023.

[15] N. Thakur, P. Kumar and A. Kumar. "A systematic review of machine and deep learning techniques for the identification and classification of breast cancer through medical image modalities". *Multimed Tools Appl*., vol. 83, pp. 35849-35942, 2024.

[16] M. Safari, A. Fatemi and L. Archambault. "MedFusionGAN: multimodal medical image fusion using an unsupervised deep generative adversarial network". *BMC Med Imaging*, vol. 23, 203, 2023.

[17] A.S. Lundervold and A. Lundervold. "An overview of deep learning in medical imaging focusing on MRI". *Z Med Phys*., vol. 29, no. 2, pp. 102-127, 2019.

[18] V, Nainamalai, M. Lippert, H. Brun, O.J. Elle and R.P. Kumar. "Local integration of deep learning for advanced visualization in congenital heart disease surgical planning". *Intell Based Med*., vol. 6, 100055, 2022.

[19] M. Akazawa and K. Hashimoto. "Artificial intelligence in gynecologic cancers: current status and future challenges – a systematic review". *Artif Intell Med*., vol. 120, 102164, 2021.

[20] V.S. de Siqueira, M.M. Borges, R.G. Furtado, C.N. Dourado and R.M. da Costa. "Artificial intelligence applied to support medical decisions for the automatic analysis of echocardiogram images: a systematic review". *Artif Intell Med*., vol. 120, 102165, 2021.

[21] T. Fernando, H. Gammulle, S. Denman, S. Sridharan and C. Fookes. "Deep learning for medical anomaly detection – a survey". *ACM Comput Surv*., vol. 54, no. 7, 2021.

[22] J. Chen J, K. Li, Z. Zhang, K. Li and P.S. Yu. "A survey on applications of artificial intelligence in fighting against COVID-19". *ACM Comput Surv*., vol 54, no. 8, 2021.

[23] M. Sah and C. Direkoglu. "A survey of deep learning methods for multiple sclerosis identification using brain mri images". *Neural Comput Appl*., vol. 34, no. 10, pp. 7349-7373, 2022.

[24] M.A. Abdou. "Literature review: efficient deep neural networks techniques for medical image analysis. *Neural Comput Appl*., vol. 34, no. 8, pp. 5791-5812, 2022.

[25] A. Kaur, L. Kaur and A. Singh. "GA-UNet: UNet-based framework for segmentation of 2D and 3D medical images applicable on heterogeneous datasets". *Neural Comput & Applic*., vol. 33, pp. 14991-15025, 2021.

[26] M.S. Hossain, G.M. Shahriar, M.M.M. Syeed, M.F. Uddin, M. Hasan, S. Shivam and S. Advani. "Region of interest (ROI) selection using vision transformer for automatic analysis using whole slide images". *Sci Rep*., vol. 13, 11314, 2023.
[27] I. Pandová, M. Rimár, A. Panda, J. Valíček, M. Kušnerová and M. Harničárová. "A study of using natural sorbent to reduce iron cations from aqueous solutions." *International Journal of Environmental Research and Public Health,* 17 (10), 3686, 2020.
[28] A. Panda, V.M. Anisimov, V.V. Anisimov, K. Dyadyura and I. Pandova. "Increasing of wear resistance of linear block-polyurethanes by thermal processing methods." *MM Science Journal*, 2021, October, pp. 4731-4735, 2021.
[29] A. Panda, M. Prislupčák and I. Pandová. "Progressive technology diagnostics and factors affecting machinability." *Applied Mechanics and Materials*, 616, pp. 183-190, 2014.
[30] R. Cantor and T.A. Curtis. "Prosthetic management of edentulous mandibulectomy patients. Part II. Clinical procedures". *J. Prosthet. Dent*., vol. 25, pp. 546-555, 1971.
[31] R. Cantor and T.A. Curtis. "Prosthetic management of edentulous mandibulectomy patients. Part III. Clinical evaluation". *J. Prosthet. Dent*., vol. 25, pp. 670-678, 1971.
[32] D. Dmitrishin, G. Lesaja, I. Skrinnik and A. Stokolos. "A new method for finding cycles by semilinear control". *Physics Letters, Section A: General, Atomic and Solid State Physics*, vol. 383, no. 16, pp. 1871-1878, 2019.

Anton Panda (corresponding author)
ORCID ID: 0000-0002-1759-7355
Technical University of Kosice
Faculty of Manufacturing Technologies
Bayerova 1, 08001 Presov, Slovakia
e-mail: anton.panda@tuke.sk

Kostiantyn Dyadyura
ORCID ID: 0000-0002-7575-9711
Department of Biomedical Engineering
Odesa Polytechnic National University
Shevchenka Ave, 1, 65044 Odesa, Ukraine
e-mail: dyadyura.k.o@op.edu.ua

Dmitriy Dmitrishin
ORCID ID: 0000-0002-2291-2364
Department of Applied Mathematics
Odessa National Polytechnic University
Shevchenka Ave, 1, 65044 Odesa, Ukraine
e-mail: dmitrishin@op.edu.ua

Andrey Smorodin
ORCID ID: 0000-0002-3370-3197
Department of Applied Mathematics
Odessa National Polytechnic University
Shevchenka Ave, 1, 65044 Odesa, Ukraine
e-mail: andrey.v.smorodin@op.edu.ua

Igor Prokopovich
ORCID ID: 0000-0002-8059-6507
Department Of Design Information Technologies and Design
Odesa Polytechnic National University
Shevchenka Ave, 1, 65044 Odesa, Ukraine
e-mail: igor.prokopovich@gmail.com